———, and T. Matsuo. "Studies on Melt Spinning. I. Fundamental Equations in the Dynamics of Melt Spinning," *J. Polymer Sci.*, part A, 3, 2541 (1965).
Marrucci, G., "The Free Energy Constitutive Equation for Polymer Solutions from the Dumbell Model," *Trans. Soc. Rheol.*, *16*, 321 (1972).
Matovich, M. A., and J. R. A. Pearson, "Spinning a Molten Threadline: Steady State, Isothermal Viscous Flows," *Ind. Eng. Chem. Fundamentals*, 8, 512 (1969).
Pearson, J. R. A., Y. T. Shah, and R. D. Mhaskar, "On the Stability of Fiber Spinning of Freezing Liquids," *Ind. Eng. Chem. Fundamentals*, **15**, 31 (1976).
Petrie, C. J. S., and M. M. Denn, "Instabilities in Polymer Processing," *AIChE J.*, **22**, 209 (1976).
Shah, Y. T., and J. R. A. Pearson, "On the Stability of Non-Isothermal Fibre Spinning," *Ind. Eng. Chem. Fundamentals*, **11**, 145 (1972).

Manuscript received August 16 and accepted October 13, 1976.

Turbulent Mass Transfer Rates to a Wall for Large Schmidt Numbers

DUDLEY A. SHAW
and
THOMAS J. HANRATTY
University of Illinois
Urbana, Illinois

New measurements are presented on the influence of Schmidt number on the rate of mass transfer between a turbulent fluid and a pipe wall. It is found that for large Schmidt numbers the fully developed mass transfer coefficient is related to the friction velocity and the Schmidt number by the equation

$$K_\infty = 0.0889\, v^* \, Sc^{-0.704}$$

The experiments are accurate enough to rule out the $Sc^{-2/3}$ or the $Sc^{-3/4}$ relations commonly used, deduced from plausible limiting expressions for the eddy diffusivity close to a wall. It is argued that these expressions are valid only over a vanishingly small portion of the concentration field as $Sc \to \infty$.

SCOPE

Mass transfer between a turbulent fluid and a solid boundary is usually characterized by a large Schmidt number Sc. For this reason, considerable attention has been given to the definition of the limiting relation for the rate of mass transfer as $Sc \to \infty$. A local mass transfer coefficient characterizing the mass transfer process can be defined as

$$K = \frac{N_0}{C_B - C_W} \tag{1}$$

In a series of very careful experiments at $Sc = 2\,400$, Son and Hanratty (1967) established that for flow in a pipe, the influence of fluid velocity on the local mass transfer coefficient is defined by the equation

$$K = v^* \, g(Sc, x^+) \tag{2}$$

For large enough values of x^+, a fully developed condition is reached where K is independent of x^+. That is

$$K_\infty = v^* \, f(Sc) \tag{3}$$

The usual procedure is to represent $f(Sc)$ as a power law

$$f(Sc) = B\, Sc^m \tag{4}$$

There has been a considerable difference in opinion as to what is the proper exponent m. The two relations most often considered are $m = -2/3$ and $m = -3/4$. These are usually justified by recognizing that the concentration boundary layer is so thin for large Sc that the velocity field within δ_c can be represented as a Taylor series expansion in terms of the dimensionless distance from the wall y^+. By using an analogy between momentum transfer and mass transfer, it is argued that the eddy diffusivity is given as $\epsilon/\nu^* \sim y^{+n}$, where n is an integer greater than or equal to 3. (See pages 343-7 of the book by Monin and Yaglom, 1965.)

In order to establish the correct exponent m, it is necessary to obtain very precise measurements over a wide range of Schmidt numbers, since the difference between the $Sc^{-2/3}$ and the $Sc^{-3/4}$ relations is not great. A considerable number of experimental studies have been directed toward this goal. However, there is enough disagreement among the results of different investigators that the problem has not been conclusively resolved.

During the course of a study on the influence of Schmidt number on the frequency of mass transfer fluctuations, we obtained the very extensive set of measurements of $f(Sc)$ presented here. Because of the care given to the execution of these experiments, we feel that a greater precision was attained than in previous investigations.

Correspondence concerning this paper should be addressed to Thomas J. Hanratty, Department of Chemical Engineering, University of Illinois, Urbana, Illinois 61801.

CONCLUSIONS AND SIGNIFICANCE

The results are surprising in that we find $m = -0.704$ rather than $-2/3$ or $-3/4$.

If it is assumed that the eddy diffusivity is given by a power law

$$\frac{\epsilon}{\nu} = b\,y^{+n} \tag{5}$$

where the coefficient is independent of Sc, then the mass transfer measurements give $b = 0.000463$ and $n = 3.38$. This relation cannot represent the limiting behavior of ϵ for small y^+, since the power n is not an integer. However, an examination of the equations for the fluctuating concentration and velocity fields shows that this is of no consequence, since the limiting relation for ϵ should be applicable only for a vanishingly small part of the concentration field as $Sc \to \infty$. It is further argued that since molecular diffusivity affects the concentration fluctuations in a vanishingly small region, it is acceptable to represent ϵ by a function independent of Sc, as was done above.

One of the consequences of these results is that for large Schmidt numbers the analogy between momentum and mass transfer does not hold in that the eddy diffusivity is not proportional to the eddy viscosity.

OUTLINE OF THE EXPERIMENTS

Two experimental methods have been used to determine $f(Sc)$ in Equation (3). One of these involves the measurement of the change of weight of a section of a soluble wall; the other involves the measurement of the electric current flowing to a section of wall which is an electrode in an electrolysis cell. Results obtained by dissolving surfaces are of uncertain reliability because, as pointed out by Linton and Sherwood (1950), small fissures and surface roughnesses can develop while the dissolution is progressing. Consequently, in recent years the electrochemical technique has been in greater favor.

Lin, Denton, Gaskill, and Putnam (1951) were the first to use electrochemical methods. They studied mass transfer for $410 < Sc < 1\,785$ to the inner wall of an annulus through which a turbulent fluid was flowing. Son and Hanratty (1967) later reinterpreted these results so as to account for entrance effects. The test electrode of the electrolysis cell used by Lin et al. was a portion of the inner wall, while the counter electrode was a portion of the outer wall located opposite the test electrode. The reactions studied were the reduction of ferricyanide on a copper cathode, reduction of quinone on a silver cathode, reduction of oxygen on a silver cathode, and oxidation of ferrocyanide on a stainless steel anode. They maintained the voltage on the test electrode in a range where it was polarized. That is, it was large enough that the reaction proceeded rapidly and $C_W \cong 0$, yet small enough that side reactions did not occur.

Van Shaw (1963) carried out the ferricyanide-ferrocyanide redox reaction in a 2.54 cm pipeline using an electrolyte with a large excess of sodium hydroxide and equimolar concentrations of ferricyanide and ferrocyanide ions. The cathode of the electrolysis cell was a section of nickel pipe located far enough from the entrance that the flow was fully developed. The anode was a much longer section of pipe located downstream from the cathode. By studying mass transfer to different lengths of pipe, he was able to determine the mass transfer coefficient under fully developed conditions. He reported $K_z^+ = 3.01 \times 10^{-4}$ for $Sc = 2\,400$, where K^+ is the local mass transfer coefficient made dimensionless with respect to the friction velocity. Later, Son and Hanratty (1967) reported that an error was made in the calibration of some of Van Shaw's orifice plates so that $K_z^+ = 3.52 \times 10^{-4}$ for $Sc = 2\,400$. They verified this result by repeating Van Shaw's experiments and by carrying out additional studies in which they measured the mass transfer rate to a small wire embedded in and ground flush with the surface of a pipe which was the cathode of an electrolysis cell. In another laboratory, Schutz (1964) carried out experiments very similar to those done by Van Shaw and obtained close agreement on the measurement of K_z^+.

Hubbard and Lightfoot (1966) carried out the ferricyanide reduction reaction in a rectangular duct for Schmidt numbers between 1 700 and 30 000 and Reynolds numbers from 7 000 to 60 000. Different Schmidt numbers were obtained by varying the temperature and the caustic concentration. The cathode was a nickel plate placed in the lower wall of the channel. The nickel anode was located directly above it. Values of m calculated from their measurements vary from an average of -0.633 at $Re = 60\,000$ to -0.700 at $Re = 7\,000$.

Mizushina et al. (1971) performed very similar measurements for Schmidt numbers from 631 to 15 500. Their method was different from Hubbard's in that instead of measuring the mass transferred to a single long cathode, they had a two-piece cathode which allowed them to measure the mass transferred to the downstream section alone. The upstream section was long enough to insure a fully developed concentration boundary layer. The measurements were in good agreement with Hubbard's and indicate that $m = -2/3$.

The experiments described in this paper were carried out in a 2.54 cm pipe using the same flow loop employed by Son (1965) and by Van Shaw (1963). Fifty measurements of the mass transfer coefficient were obtained for Schmidt numbers ranging from 693 to 37 200. Two different electrolysis systems were used. One of these consisted of potassium ferrocyanide, potassium ferricyanide, and a large excess of sodium hydroxide dissolved in water. The other consisted of iodine and a large excess of potassium iodide dissolved in a water-sucrose solution. The Schmidt number was varied by either changing the sodium hydroxide concentration or the sucrose concentration. The cathode was a section of brass pipe which was plated with platinum. The plated metal provided a very smooth surface so that the influence of wall roughness was minimized.

The value of the fully developed mass transfer coefficient was determined by comparing the mass transfer rates to cathodes with different lengths under the same flow conditions. Measurements of K_z^+ were also made with small wire electrodes embedded in the downstream end of the cathode.

THEORY

The Use of Eddy Diffusion Coefficients

Theoretical guidance for the correlation of turbulent mass transfer coefficients has been obtained by solving the mass balance equation using an eddy diffusion coefficient $\epsilon(y)$. In this approach, the mass flux to a plane perpendicular to the y axis N is given by

$$N = -[D + \epsilon(y)]\frac{d\overline{C}}{dy} \tag{6}$$

The usual procedure is to represent the eddy diffusivity as

$$\frac{\epsilon}{\nu} = b(Sc)\, y^{+n} \tag{5}$$

where y^+ is the distance from the wall made dimensionless using the friction velocity and the kinematic viscosity of the fluid. Son and Hanratty (1967) have shown that the solution of the mass balance equation at high Schmidt numbers using (4) gives

$$K_x^+ = \frac{n}{\pi} b^{\frac{1}{n}} \sin\left(\frac{\pi}{n}\right) Sc^{-\left(\frac{n-1}{n}\right)} \tag{7}$$

The dependency of K_x^+ on Sc can then be related to the exponent n and the influence of Schmidt numbers on the coefficient b.

Since for $Sc \to \infty$ the thickness of the concentration boundary layer becomes vanishingly small, the velocity field influencing the variation of $\epsilon(y)$ can be represented by the first term of a Taylor series in y. Thus, as shown in pages 279-282 of the book by Monin and Yaglom (1965) the time average, the component of the turbulent velocity fluctuations perpendicular to the wall, and the turbulent eddy viscosity are given as

$$\overline{U} = v^* y^+ \tag{8}$$

$$v' = (\overline{v}^2)^{1/2} = k_1 v^* y^{+2} \tag{9}$$

$$\frac{\nu_T}{\nu} = k_2 y^{+3} + k_3 y^{+4} \tag{10}$$

If it is assumed that turbulent mass transport is analogous to momentum transport in that ϵ is proportional to ν_T, then it would follow that either $\epsilon \sim y^{+3}$ or $\epsilon \sim y^{+4}$, depending on whether $k_2 = 0$.

Another theoretical approach for estimating the exponent in (4) is to use a Taylor series expansion of the concentration field as well as the velocity field. Then

$$c' = (\overline{c}^2)^{1/2} = k_4 \frac{d\overline{C}}{dy}\bigg|_{\text{wall}} y \tag{11}$$

where k_4 is a proportionality constant. The eddy diffusivity can be related to the fluctuating concentration and velocity field by using a Reynolds transport coefficient

$$\overline{vc} = -\epsilon(y)\frac{d\overline{C}}{dy} \tag{12}$$

Since

$$\overline{vc} = R\, v'\, c' \tag{13}$$

where R is the correlation coefficient for $y \to 0$, it follows that the limiting behavior of $\epsilon(y)$ for $y \to 0$ is

$$\epsilon^+ = \frac{\epsilon(y)}{\nu} = -R\, k_1 k_4\, y^{+3} \tag{14}$$

A number of researchers have assumed that (14) is valid throughout the concentration field and that the correlation coefficient R is independent of Schmidt number to argue from (7) that $K_x^+ \sim Sc^{-2/3}$.

Levich (1962) has taken a slightly different approach. He has assumed that

$$c' = k_5 v' \Upsilon \frac{d\overline{C}}{dy} \tag{15}$$

where Υ is a time constant characterizing the velocity fluctuations in the immediate vicinity of the wall, and k_5 is a proportionality constant. Then

$$\overline{vc} = R\, k_1^2\, k_5\, v^{*2}\, \Upsilon \frac{d\overline{C}}{dy} y^{+4} \tag{16}$$

or

$$\epsilon^+ = R k_1^2\, k_5\, T^+\, y^{+4} \tag{17}$$

where $T^+ = Tv^{*2}/\nu$. Levich assumed that the correlation coefficient R is independent of Sc to argue that $\epsilon^+ \sim y^{+4}$ and from (7) that $K_x^+ \sim Sc^{-3/4}$.

Criticism of the Assumption that $\epsilon(y)$ is Given by the Limiting Value for $y \to 0$

The assumption that $\epsilon(y)$ is given by the limiting value for $y \to 0$, Equation (14), does not appear to be consistent with present knowledge regarding the concentration field. The reason for this is that the region over which the limiting relation is valid, δ_L, becomes vanishingly small compared to the thickness of the concentration boundary, δ_c, layer as $Sc \to \infty$.

The thickness δ_c can be defined by

$$\delta_c^+ = \frac{1}{K^+ Sc} \tag{18}$$

where $\delta_c^+ = \delta_c v^*/\nu$. Consequently, $\delta_c^+ \sim Sc^{-p}$, with $1/4 < p < 1/3$. The differential equation describing the concentration fluctuation is obtained from the mass balance equation as indicated by Hinze (1959):

$$\frac{\partial c}{\partial t} + \overline{U}\frac{\partial c}{\partial x} + v\frac{d\overline{C}}{dy} + u\frac{\partial \overline{C}}{\partial x} = D\left(\frac{\partial^2 c}{\partial y^2} + \frac{\partial^2 c}{\partial x^2} + \frac{\partial^2 c}{\partial z^2}\right) - \frac{\partial}{\partial x}(uc) - \frac{\partial}{\partial y}(vc - \overline{vc}) - \frac{\partial}{\partial z}(wc) \tag{19}$$

The orders of magnitude of several of the terms appearing in this equation have been examined by Sirkar and Hanratty (1970). They showed that for large Schmidt numbers, $\partial^2 c/\partial y^2$ is large compared to $\partial^2 c/\partial x^2$ and $\partial^2 c/\partial z^2$ and that $\partial c/\partial t$ is large compared to $\overline{U}(\partial c/\partial x)$ or $u(\partial \overline{C}/\partial x)$. Equation (19) then simplifies to

$$\frac{\partial c^+}{\partial t^+} + v^+\frac{d\overline{C}^+}{dy^+} = \frac{1}{Sc}\left(\frac{\partial^2 c^+}{\partial y^{+2}}\right) - \frac{\partial}{\partial x^+}(u^+c^+) - \frac{\partial}{\partial z^+}(w^+c^+) - \frac{\partial}{\partial y^+}(v^+c^+ - \overline{v^+c^+}) \tag{20}$$

where t, y, u, v, and w have been made dimensionless using wall parameters v^* and ν. $\overline{C}$ and c have been made dimensionless using C_B. The term $(1/Sc)(\partial^2 c^+/\partial y^{+2})$ which governs the influence of molecular diffusion should be of prime importance close to the wall and therefore should play a role in determining the limiting behavior of $\overline{vc}$ as $y \to 0$. Since the transient term $\partial c^+/\partial t^+$ is of the same order as $(1/Sc)(\partial^2 c^+/\partial y^{+2})$ close to the wall, we conclude that the thickness of the region over which the limiting relation for the eddy diffusivity is valid has the dependency

$$\delta_L^+ \sim Sc^{-1/3} \tag{21}$$

Since $\delta_c^+ \sim Sc^{-1/3 \text{ or } -1/4}$, it follows that $\delta_L^+/\delta_c^+ \to 0$ as $Sc \to \infty$.

The above conclusion can be illustrated by solving the form of (20) that is linear in the fluctuating quantities:

$$\frac{\partial c^+}{\partial t^+} + v^+ \frac{d\bar{C}^+}{dy^+} = \frac{1}{Sc}\left(\frac{\partial^2 c^+}{\partial y^{+2}}\right) \tag{22}$$

This will be done for the case of a harmonic variation v^+

$$v^+ = \hat{v} y^{+2} e^{i\omega^+ t^+} \tag{23}$$

The term

$$\frac{d\bar{C}^+}{dy^+} = \frac{\bar{K}^+}{\frac{1}{Sc} + \epsilon^+} \tag{24}$$

since the mass flux does not vary significantly through the concentration boundary layer for $Sc \to \infty$. The solution of (22) can be expected to be of the form

$$c^+ = \hat{c}\, e^{i\omega^+ t^+} \tag{25}$$

so that (22) becomes

$$i\omega^+ \hat{c} + \hat{v} y^{+2} \frac{d\bar{C}^+}{dy^+} = \frac{1}{Sc} \frac{\partial^2 \hat{c}}{\partial y^{+2}} \tag{26}$$

For small y^+, where the amplitude $\hat{c}$ varies linearly with y^+, the term $i\omega^+ \hat{c}$ is of the same order as $(1/Sc)(\partial^2 \hat{c}/\partial y^{+2})$. For large y^+, the molecular diffusion term is negligible and $\hat{c}$ varies in a way similar to that suggested by Levich in (15):

$$\hat{c} = -\frac{\hat{v}}{i\omega^+} y^{+2} \frac{d\bar{C}^+}{dy^+} \tag{27}$$

A solution to (26) has been presented by Shaw (1976) and by Shaw and Hanratty (1977) for the boundary conditions that $\hat{c} = 0$ at $y^+ = 0$ and as $y^+ \to \infty$. The amplitude of the concentration fluctuations is given as $|\hat{c}| = (\hat{c}\,\hat{c}^*)^{1/2}$, where c^* is the complex conjugate of c. The ratio $\dfrac{|\hat{c}|}{|\hat{v}| \dfrac{d\bar{C}^+}{dy^+}}$ calculated from (26) for $\omega^+ = 0.0628$ and for $\epsilon^+ = 0.00032 y^{+4}$ is shown in Figure 1, where the distance from the wall has been normalized with respect to $\delta_c^+ \sim (1/Sc^{1/4})$. The value of ω^+ used in this calculation was taken as the median frequency of the fluctuations of u in the viscous sublayer determined from the measurements of Lee (1968). The calculated amplitude was found to be independent of the form chosen for ϵ^+. The same profile was obtained for $\epsilon^+ = 0.000463 y^{+3.38}$.

One of the results of this calculation is that as $y^+ \to 0$

$$\overline{v^+ c^+} = -\sqrt{2}\, Sc^{1/2}\, \bar{K}^+\, y^{+3} \int_0^\infty \frac{W_v}{\omega^{+3/2}}\, d\omega^+ \tag{28}$$

or that

$$\epsilon^+ = \frac{\sqrt{2}\, y^{+3}}{Sc^{1/2}} \int_0^\infty \frac{W_{\hat{v}}}{\omega^{+3/2}}\, d\omega^+ \tag{29}$$

This is consistent with (14), but, contrary to the assumption usually made, the coefficient is found to depend on Schmidt number. The solid line in Figure 1 is (27),

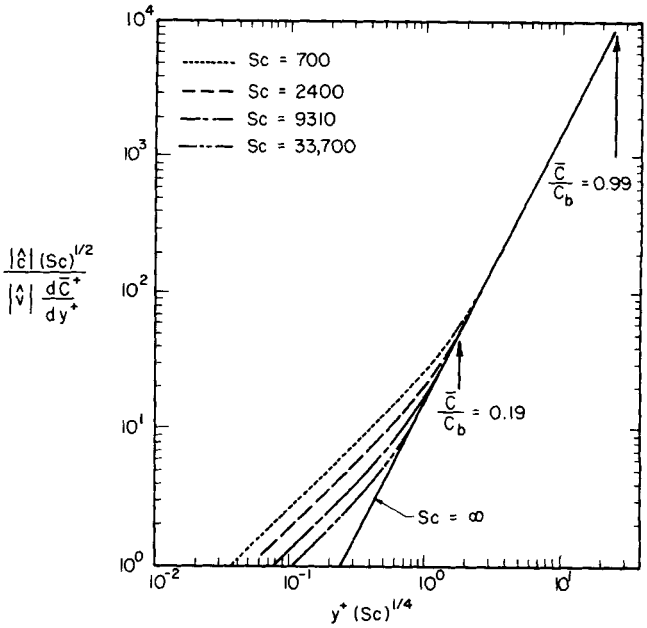

Fig. 1. Amplitude of the concentration fluctuations calculated from the linearized equation.

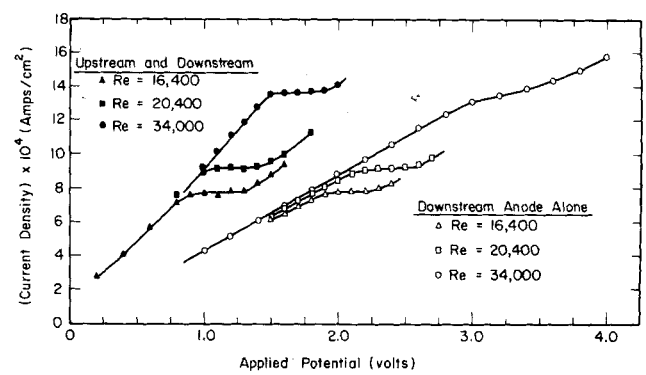

Fig. 2. Polarization curves for different anode configurations at $Sc = 695$.

and the broken lines represent the region where the concentration fluctuations are affected by molecular diffusion. These show the linear dependency on y^+ at small y^+ given by (11). If the edge of the concentration boundary layer is defined as $\bar{C}/C_b = 0.99$, then it is located at the value of $y^+(Sc)^{1/4}$ indicated by the arrow in Figure 1. From Figure 1 it is seen that the fraction of the concentration boundary layer over which molecular diffusivity is influencing the concentration fluctuations becomes progressively smaller as the Schmidt number increases.

Of particular interest is the result that for $Sc \to \infty$ the variation of the concentration fluctuation over almost all of the concentration boundary layer is not influenced by molecular diffusion. That is, it is given by (27). This would suggest that the eddy diffusion coefficient for $Sc \to \infty$ should be represented by an equation of the form

$$\epsilon^+ = g(y^+) \tag{30}$$

If the simplified version of the mass balance Equation (22) were valid, we would get

$$g(y^+) \sim y^{+4} \tag{31}$$

as suggested by Levich. However, there is no reason to expect that the nonlinear terms in (20) are negligible for large y^+. Consequently, we must anticipate that $g(y^+)$ could be more complicated than the Levich relation.

DESCRIPTION OF EXPERIMENTS

Electrochemical System

The electrochemical reactions used in the mass transfer measurements are as follows:

Test electrode (cathode) $I_3^- + 2e^- \rightarrow 3I^-$

Reference electrode (anode) $3I^- \rightarrow I_3^- + 2e^-$

Test electrode (cathode)

$$Fe(CN)_6^{3-} + e^- \rightarrow Fe(CN)_6^{4-}$$

Reference electrode (anode)

$$Fe(CN)_6^{4-} \rightarrow Fe(CN)_6^{3-} + e^-$$

Detailed discussions of the application of these reaction systems to measure mass transfer rates are contained in theses by Van Shaw (1963), McConaghy (1974), and Shaw (1973).

The electric current flowing through the system was measured for different voltages to obtain curves of the type shown in Figure 2. The test electrode is determined to be polarized when the electric current is in the plateau region. The mass transfer coefficient is calculated from this current by the equation

$$K = \frac{I}{n_e F A C_B} \tag{32}$$

If the pipe that constitutes the cathode of the electrolysis cell is long enough so that entrance effects are negligible, the average value of the mass transfer coefficient measured over this surface $<K>$ would be the same as the local fully developed mass transfer coefficient K_∞. In practice it is difficult to use a pipe electrode long enough so that $<K> = K_\infty$ because for a very long electrode, large voltage drops in the solution over the length of the pipe do not allow the whole cathode surface to be held at a sufficiently narrow range of voltages that it is completely polarized.

The method for getting around this difficulty used by McConaghy (1974) and by Son (1965) is to measure the current to a wire electrode embedded in the downstream end of the pipe cathode. These investigators found that the mass transfer coefficient reaches its fully developed value a short distance from the entrance to the mass transfer section, that is, $x^+ > 1\,000$, and that a relatively short cathode is required to obtain K_∞ by direct measurements with embedded electrodes.

A different method was used in the research reported in this paper for the primary measurement of K_∞ because the surface area of an embedded electrode is very difficult to measure and because the electric current from an embedded electrode can be so small that it is difficult to measure accurately.

The method employed to measure K_∞ involved measuring the current to two electrodes of different lengths in separate experiments at the same flow rate. On the assumption that at the downstream end of the shorter electrode the local value of $K = K_\infty$, then

$$K_\infty = \frac{I_{long} - I_{short}}{n_e F C_B (A_{long} - A_{short})} \tag{33}$$

For the iodine system, the long electrode was 10.8 cm and the short was 5.72 cm. Because of the high conductivity of the ferricyanide solution at high sodium hydroxide concentrations, it was possible to polarize an even longer electrode than was possible with the iodine system. The 10.8 and 5.72 cm lengths of pipe were placed together making an electrode 16.52 cm long. The two sections were electrically insulated from one another so that the currents to each part could be measured separately or the electrodes could be put together as one long electrode. It was then possible to measure K_∞^+ by the following two methods: from the difference of current of the 16.52 and 10.8 cm electrodes or from the downstream (5.72 cm) part, K_∞^+ could be measured directly. The two methods are compared in Table 1. No difference can be discerned in the results. The values for K_∞^+ reported were measured by the second method.

In the experiments performed previously in this laboratory by Van Shaw and by Son, the anode was located downstream of the cathode. In all the experiments described in this paper, the anode consisted of sections of pipe located both upstream and downstream of the cath-

TABLE 1. COMPARISON OF MEASURED VALUES K_∞^+

Run	Sc	Embedded electrode size	x^+	Embedded electrode	$K^+ \times 10^4$ 6½ (downstream portion) electrode	Difference of two electrodes
10	1 730	0.0083	3 050	4.75		4.72
13	2 460	0.005	3 600	3.59*		3.56
14	3 470	0.005	3 800	2.91*		2.81
15	5 070	0.005	4 740	2.15*		2.21
16	7 550	0.005	3 900	1.44*		1.58
17	11 700	0.0253	4 300	1.24		1.22
		0.0159	4 300	1.20		
43	12 100				1.25	1.35
44	12 100				1.23	1.31
45	15 400				0.971	0.921
12	16 900	0.0253	2 070	1.08		0.971
		0.0083	2 070	1.06		
46	20 200				0.824	0.818
47	25 800				0 673	0.621
48	25 800				0.668	0.713
49	31 800				0.614	0.580
50	33 700				0.580	0.626
3	37 200	0.0253	1 680	0.552		0.556
		0.0159	1 680	0.525		
		0.0083	1 680	0.531		

* Average from eight electrodes.

ode. This insured that the entire surface of the cathode was polarized under circumstances when the conductivity of the solution was low. Experiments were conducted to test whether the upstream anode had an effect on the measured current. Figure 2 shows current-potential curves for the two configurations. There is no difference in the current measured at the plateau for the measurements at $Re = 16\,400$ and $Re = 20\,400$. At $Re = 34\,000$, the cathode was not entirely polarized when the downstream anode is used alone, which points out the main reason for using the upstream anode.

There are some practical difficulties which limited the range of Schmidt numbers that could be studied with the two electrolysis systems.

The Schmidt number of the iodine solution was increased by increasing the sucrose content and consequently the resistance of the solution. When the voltage drop along the length of the electrode is greater than the width of the current-voltage plateau, the electrode does not become polarized at all. Therefore, it was necessary to use very low concentrations of I_2 at high Schmidt numbers. The flat portion of the polarization curve is much better defined for the lower iodine concentration. For high Reynolds numbers and Schmidt numbers, a good plateau could not be obtained even at low iodine concentrations. For extreme conditions, the measurements had to be made at an inflection point of the polarization curve. Because of this limitation, the highest Schmidt number that could be studied with the iodine electrolyte was 37 200.

Solutions of the ferricyanide electrolyte showed a reddish precipitate on standing for several days. Kolthoff and Furman (1928) note that ferricyanide ions decompose in basic solutions according to the following reaction:

$$2Fe(CN)_6^{3-} + 6(OH)^- \rightleftarrows 2Fe(OH)_3 + 12CN^-$$

The effect increases with increasing alkalinity. Because of this, it was not possible to work at concentrations of sodium hydroxide higher than 7 molar. Therefore, the highest Schmidt number that could be studied with this system was 33 700.

Flow Loop

The apparatus used to carry out the experiments is shown schematically in Figure 3. The principal elements were the test section which was the cathode for the electrolysis reaction and the two anodes. The upstream anode was a 44.5 cm length, and the downstream anode was a 152 cm length of 2.54 cm I.D. schedule 40 nickel pipe. The upstream anode was preceded by a 427 cm long entrance section made from 3.81 cm O.D. Lucite pipe. The remainder of the flow loop was constructed of 2.54 cm I.D. Ace-Ite PVC plastic pipe. The electrolyte was held in a reservoir constructed of type 304 stainless steel. The temperature of the fluid in the reservoir was controlled to within ± 0.1°C of 25°C by a laboratory temperature controller which activated a solenoid valve in a cooling water line. The electrolyte was purged with nitrogen before and during each experiment to clear the solution of dissolved oxygen. A blackened lid was placed on top of the storage tank to keep out light.

The iodine solution was circulated through the system by a Moyno pump operated at either 300 or 900 rev/min. Since the rubber stator of the Moyno pump would swell in solutions of sodium hydroxide, it was necessary to use a 316 stainless steel centrifugal pump for the experiments with ferricyanide solutions. The flow rate to the test section was regulated by recycling part of the pump discharge back to the electrolyte reservoir.

The flow rate was measured with one of two rotameters with stainless steel floats which covered a flow range from

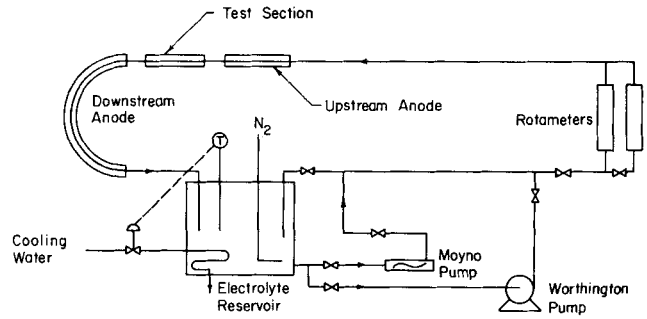

Fig. 3. Flow system.

0.019 to 2.34 l/s of water. Since the rotameter reading depends on the density of the solution, each rotameter was calibrated for a number of solutions of different density. During each experiment, the density of the solution was measured so as to determine a correction to the rotameter reading. The measured corrections agreed with the theoretical prediction for flow through an annulus (see *Theory of the Flowrator*).

Measurement of Physical Properties

The kinematic viscosity of each solution was determined within ± 0.1% by using a Cannon-Fenske viscometer (1949 Book of ASTM Standards, Part 5, page 899). For kinematic viscosities below 0.03 cm²/s, a size 50 viscometer was used. It was calibrated at 25°C with deionized water. For viscosities above 0.03 cm²/s, a size 100 viscometer was used. It was calibrated at 25°C with a solution of glycerine and water. The viscosity of this solution was first determined in the size 50 viscometer and then used to calibrate the size 100 viscometer. The measurement was repeated three times for each solution. If the individual measurements differed by more than 0.1%, the measurement was repeated until three values agreed.

The diffusion coefficient for the iodine system was measured for four sucrose concentrations using the electrochemical technique in a rotating cylinder Couette flow apparatus built by Fortuna (1971). When the rotating cylinder is operated under laminar flow conditions, the velocity gradient at the wall is known. The diffusion coefficient of the iodine in the solution can then be related to the current to a small wire embedded in the wall of the cylinder.

These four measurements were combined with twelve measurements by Newson and Riddiford (1961) obtained using diaphragm cells to yield an expression for the diffusion coefficient as a function of the kinematic viscosity of the fluid

$$D = (7.446 \times 10^{-8})\, \nu^{-1.054} \tag{34}$$

The above expression is a least-square power curve fit to the measurements. It has a coefficient of determination $r^2 \doteq 0.997$.

The diffusion coefficient of ferricyanide was calculated from the following expression proposed by Gordon, Newman, and Tobias (1966)

$$\frac{D\mu}{T} = [(0.234 + 0.0014\,\Gamma) \pm 0.005] \times 10^{-9}\, \frac{\text{cm}^2}{\text{s}}\, \frac{\text{poise}}{^\circ\text{K}} \tag{35}$$

where Γ is defined by

$$\Gamma = \frac{1}{2} \sum_{i=1}^{m} C_i \gamma_i^2 \tag{36}$$

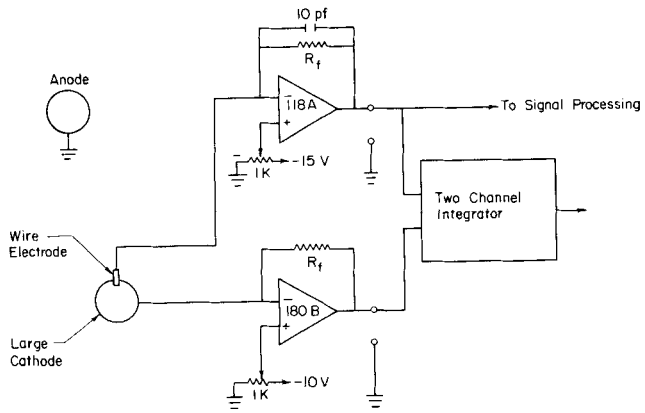

Fig. 4. Electronic circuit for mass transfer measurement.

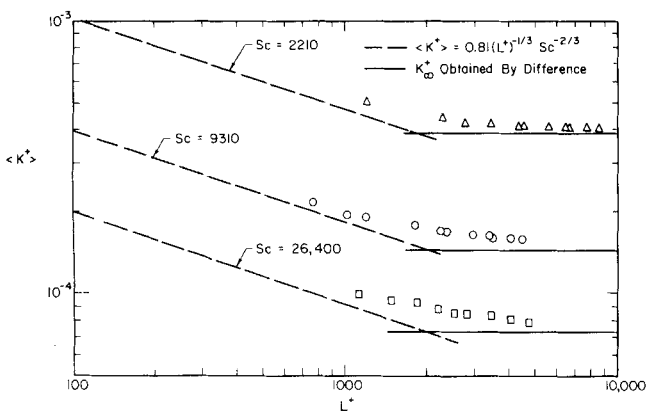

Fig. 5. Entry region for turbulent mass transfer.

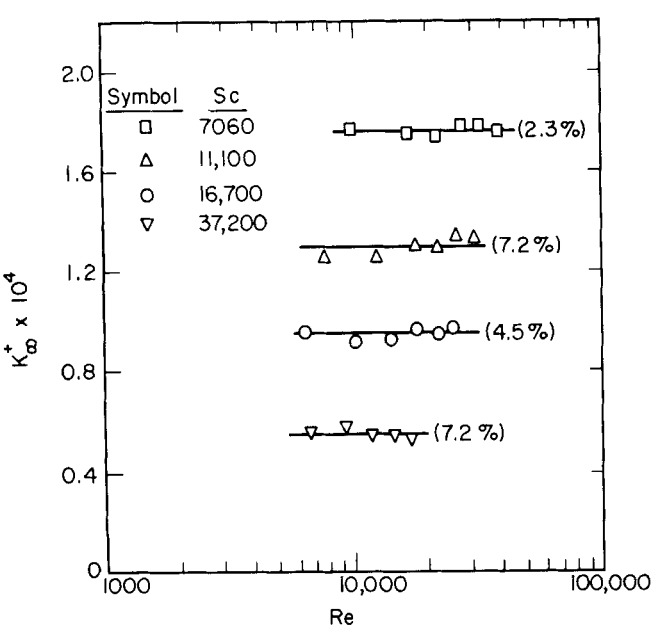

Fig 6. K_z^+ measured by difference of current (high Schmidt numbers).

where C_i is the concentration of species i, and γ is its charge. This expression was found to hold for 10M sodium hydroxide by Eckelman (1971) using the rotating cylinder apparatus.

The concentration of iodine was determined by titrating with a standard sodium thiosulphate solution with potentiometric indication. The concentration of ferricyanide was obtained by titrating with isoniazid (isonicotinic acid hydrazide) with potentiometric indication (see Hicks and Pagotto, 1974; Vulterin and Zyka, 1963). The density of the solutions was determined with a Fischer and Porter hydrometer.

The Test Section

Three test sections of 2.54 cm I.D. brass pipe plated with platinum were used. They had lengths of 10.8, 5.72, and 2.54 cm. All three sections were used in a study of the entry length for mass transfer. Once the length necessary for fully developed mass transfer was established, only the two longer sections were used to measure the overall mass transfer coefficient. After finishing and plating, the inside diameter of the test sections was 2.64 cm.

The two longer sections contained small wire electrodes to study local mass transfer rates. The test electrodes fitted to short entry and exit sections of 3.81 cm O.D. Plexiglas tubing. Great care was taken to insure that there were no discontinuities in the cross section of the pipe immediately upstream and downstream of the electrode.

The inside walls of the brass test sections were sanded with emery paper to remove roughness resulting from machining. Then the circular platinum wires used for local mass transfer measurements were glued into holes in the wall with epoxy cement. After the cement had completely cured, the inside surface was sanded with successively finer grades of silicon carbide paper to remove excess epoxy and to give the surface a very smooth finish. Finally, the surface was polished with polishing compound and Brasso. The test section was then plated with platinum (Shaw, 1973).

Electrical Circuits

The electrical circuit used for mass transfer measurements is shown in Figure 4. An Analog Devices 180 B operational amplifier, modified for large currents and operating as a current to voltage converter, was used to measure the current to the electrode. Each of the circular platinum wires used for local mass transfer measurements had its own circuit with an Analog Devices 118 A operation amplifier.

The potential applied to the cathode was determined by the setting of the 1KΩ helipot. Both upstream and downstream anodes were grounded to the amplifier ground and to the building cold water line.

The average D.C. level of the signal from the large cathode was determined by integrating the signal for 100 s using an analogue integrator which employed a timer based on a 1 MHz crystal oscillator.

RESULTS

Influence of the Length of Mass Transfer Section

Measurements of the effect of L^+ on the average mass transfer coefficient over the whole transfer surface $\langle K^+ \rangle$ were obtained by using two different electrode lengths and by varying the flow rate and therefore the friction velocity. Values of $\langle K^+ \rangle$ obtained with the iodine system are plotted in Figure 5 for different Schmidt numbers. The dashed line in the figure is the asymptotic solution for small L^+ derived by Son and Hanratty (1967):

$$\langle K^+ \rangle = 0.81(L^+)^{-1/3}\, Sc^{-2/3} \qquad (37)$$

As had previously been found by Van Shaw (1963) and by Son (1965), the results of this research show that $L^+ > 10\,000$ is needed in order that $\langle K^+ \rangle = K_\infty^+$.

Measurements of K_∞^+

Typical results on K_z^+ for the iodine system obtained from the difference in the mass transfer rate to electrodes of different length are shown in Figures 6 and 7. As had been previously indicated by Son and Hanratty (1967),

K_∞^+ is found to be independent of Reynolds number. For each of the Schmidt numbers shown in Figures 6 and 7, a value of K_∞^+ can be determined as the average of the measurements for several Reynolds numbers. Such a procedure was followed in determining each of the fifty values of K_∞^+ reported in this paper.

A few local values of the mass transfer coefficient were also measured from embedded wire electrodes in the 5.72 and 10.8 cm test sections. The results of these measurements are presented in Table 1, where x^+ is the dimensionless distance of the wire from the upstream edge of the large electrode. The table shows that even for the lowest value of $x^+ = 1\,680$, the local value of K^+ agrees with the value of K_∞^+ measured from the difference in currents to two electrodes of different lengths.

The above discussion indicates that the local mass transfer coefficient becomes fully developed for $x^+ >$ ca 1 000. For this reason, values of K_∞^+ were calculated from different measurements only for experiments in which the dimensionless length of the shorter electrode was greater than 821.

All fifty measurements of $\overline{K}_\infty^+$ are presented in Figure 8. Statistical analysis of the measurements yielded

$$\overline{K}_\infty^+ = 0.132\ Sc^{-3/4}$$

$$\sigma^2 = 7.3 \times 10^{-10} \tag{38}$$

$$\overline{K}_\infty^+ = 0.0889\ Sc^{-0.704 \pm 0.013}$$

$$\sigma^2 = 1.02 \times 10^{-10} \tag{39}$$

$$\overline{K}_\infty^+ = 0.0649\ Sc^{-2/3}$$

$$\sigma^2 = 6.14 \times 10^{-10} \tag{40}$$

The coefficient of correlation for the measurements was $r^2 = 0.999$. The limits shown for the exponent in Equation (39) are for 99.9% confidence. The ratios of the mean square errors of the $-3/4$ and $-2/3$ relation to the mean square error of Equation (39) show that Equation (39) is a significantly better relation than either the $-2/3$ or the $-3/4$ relation.

The measurement from each electrolyte were analyzed separately to obtain the following relations:

$$\text{Iodine:}\quad K_\infty^+ = 0.0861\ Sc^{-0.699} \tag{41}$$

$$\text{Ferricyanide:}\quad K_\infty^+ = 0.0955\ Sc^{-0.712} \tag{42}$$

Both exponents are within the specified range of the exponent in Equation (39).

We have also checked whether (39) is the best representation over the whole range of Schmidt numbers studies. This was done by obtaining least-square approximations to the data in the low and high Schmidt number ranges. The equations are

$$693 \leq Sc \leq 5\,070 \tag{43}$$

$$K_\infty^+ = 0.0978\ Sc^{-0.716}$$

$$6\,080 \leq Sc \leq 37\,200 \tag{44}$$

$$K_\infty^+ = 0.0861\ Sc^{-0.700}$$

Since both exponents are within the confidence levels of Equation (39), it is concluded that there is no significant difference in slope between the low and high ranges of Schmidt numbers covered by the data.

Comparison with Measurements from Other Laboratories

Figure 9 compares the measurements made for this study to those of other investigators. The values of K_∞^+ measured by several people using the electrochemical technique agree for large Schmidt numbers, but, below a

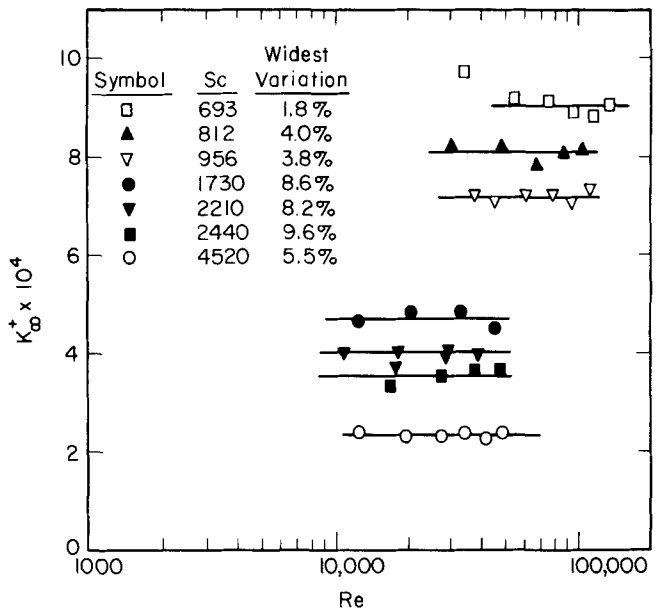

Fig. 7. K_∞^+ measured by difference of current (low Schmidt numbers).

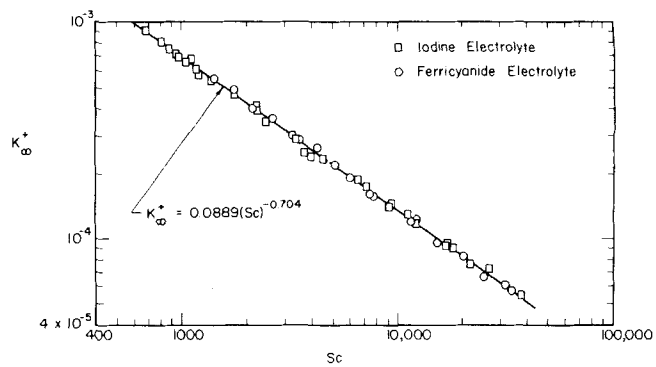

Fig. 8. Results of average mass transfer measurements.

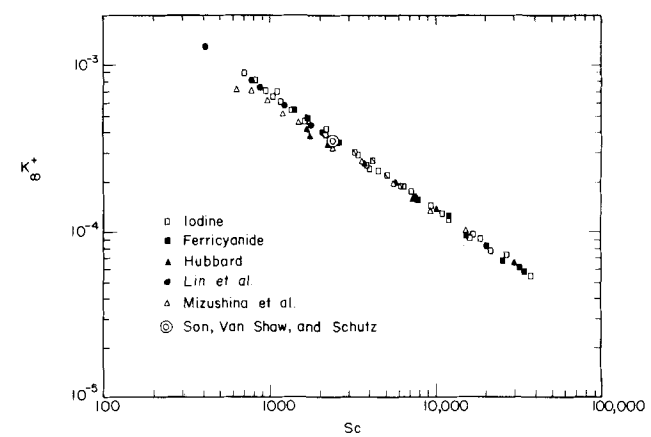

Fig. 9. Comparison of electrochemical mass transfer measurements.

Schmidt number of about 3 000, the values obtained by Mizushina et al. (1971) in channel flow and by Hubbard (1964) in channel flow are lower than the measurements made by Lin et al. (1951) for flow in an annulus and the measurements made in a pipe. Note that the results of Son (1965), Van Shaw (1963), and Schutz (1964) for pipe flow agree so well that they are represented by only one point on the graph. The reason for the difference between the data in pipe flow and channel flow is not understood.

DISCUSSION

From presently available measurements, we conclude that over the Schmidt number range 700 to 37 000 the fully developed mass transfer coefficient for a pipe is given by the equation

$$K_\infty^+ = 0.0889\ Sc^{-0.704} \tag{39}$$

In order for this to be consistent with either of the eddy diffusivity relations

$$\epsilon^+ = b_3\, y^{+3} \tag{45}$$

or

$$\epsilon^+ = b_4\, y^{+4} \tag{46}$$

it is necessary that

$$b_3 = 0.001\,242\ Sc^{-0.112} \tag{47}$$

or that

$$b_4 = (9.51 \times 10^{-5})\ Sc^{0.184} \tag{48}$$

We prefer to use an eddy diffusivity relation for $Sc \to \infty$ which is independent of Schmidt number. Consequently, we would interpret (39) as suggesting

$$\epsilon^+ = 0.000463\ y^{+3.38} \tag{49}$$

It is evident that an explanation of this relation through solutions of the mass balance Equation (19) will require a modeling of the nonlinear terms. This presents a considerable challenge for further theoretical work on this problem.

ACKNOWLEDGMENT

This work was partially supported by the National Science Foundation under Grant NSF ENG 71-02362.

NOTATION

A = surface area of cathode, cm^2
B = constant defined in Equation (4)
b = constant defined in Equation (5)
b_3 = constant defined in Equation (39)
b_4 = constant defined in Equation (40)
$\overline{C}$ = time averaged concentration, moles/cm^3
C^+ = $(C - C_w)/(C_B - C_w)$
C_B = bulk averaged concentration, moles/cm^3
C_w = concentration at the wall, moles/cm^3
c = fluctuating component of the concentration, moles/cm^3
c' = root-mean-square of c, moles/cm^3
$\hat{c}$ = amplitude of the concentration fluctuations
D = molecular diffusion coefficient, cm^2/s
d = hydraulic diameter, cm
F = 96 500 coul/equiv, Faraday's constant
I = current, amp
K = mass transfer coefficient, cm/s
K_∞ = fully developed mass transfer coefficient, cm/s
K^+ = K/v^*
K_∞^+ = K_∞/v^*
k_i = constants used in Equations (9), (10), (11), (15)
L = length of electrode, cm
L^+ = Lv^*/ν
m = exponent in Equation (4)
N = mass flux to a plane perpendicular to the y axis, moles/cm^2 s
N_0 = local mass flux to the wall, moles/cm^2 s
n = exponent in Equation (5)
n_e = number of electrons exchanged in the reduction reaction
p = $m + 1$
r = coefficient of correlation t_v
R = correlation coefficient $\overline{vc}/v'c'$ for $y \to 0$
Re = $u_b d/\nu$, Reynolds number
Sc = ν/D, Schmidt number
t = time, s
t^+ = tv^{*2}/ν
T = time constant characterizing velocity fluctuations in immediate vicinity of wall, s
T^+ = Tv^{*2}/ν
$\overline{U}$ = time averaged streamwise velocity, cm/s
u = fluctuating velocity component in the mean flow direction, cm/s
u_b = bulk averaged velocity, cm/s
v = fluctuating velocity component in the direction normal to the wall, cm/s
v' = root-mean-square of v, cm/s
$\hat{v}$ = amplitude of the v velocity fluctuations
v^* = friction velocity, cm/s
$W_{\hat{v}}$ = spectrum of the v velocity fluctuations, cm^2/s
w = component of the fluctuating velocity in the z direction, cm/s
x = coordinate in direction of mean flow, cm
x^+ = dimensionless distance from the upstream edge of the mass transfer section
y = coordinate direction normal to pipe wall, cm
y^+ = yv^*/ν
z = coordinate direction transverse to the mean flow, cm

Greek Letters

γ = valence of an ion
Γ = ionic strength defined by Equation (36)
δ_c = thickness of the concentration boundary layer, cm
δ_c^+ = $\delta_c v^*/\nu$
δ_L^+ = dimensionless thickness of the region over which molecular diffusion is important
ϵ = eddy diffusion coefficient, cm^2/s
ϵ^+ = ϵ/ν
ν = kinematic viscosity, cm^2/s
ν_T = turbulent eddy viscosity, cm^2/s
σ^2 = mean square error
ω^+ = $\omega\nu/v^{*2}$, dimensionless circular frequency

LITERATURE CITED

Eckelman, L. D., Ph.D. thesis, Univ. Ill., Urbana (1971).

Fortuna, G., Ph.D. thesis, Univ. Ill., Urbana (1971).

Gordon, S. L., "Investigation of Ionic Diffusion and Migration by a Rotating Disk Electrode," M. S. thesis, Univ. Calif. (1963).

———, J. S. Newman, and C. W. Tobias, "The Role of Ionic Migration in Electrolytic Mass Transport; Diffusivities of $[Fe(CN)_6]^{3-}$ and $[Fe(CN)_6]^{4-}$ in KOH and NaOH Solutions," *Ber. Bunsenges. Physik. Chem.*, **70**, 414, (1966).

Hicks, R. E., and N. Pagotto, "The Effect of Drag Reducing Polymers and Plastics on the Ferricyanide Concentration in Electrolyte Solutions Used in Mass Transfer Determinations," *CSIR Report CENG M-024*, Pretoria, South Africa (1974).

Hinze, J. O., *Turbulence*, McGraw-Hill, New York (1959).

Hubbard, D. W., "Mass Transfer in Turbulent Flow at High Schmidt Numbers," Ph.D. thesis, Univ. Wisc., Madison (1964).

———, and E. N. Lightfoot, "Correlation of Heat and Mass Transfer Data for High Schmidt and Reynolds Numbers," *Ind. Eng. Chem. Fundamentals*, **5**, 370 (1966).

Kolthoff, I. M., and N. H. Furman, *Volumetric Analysis*, Vol. I, p. 231, J. Wiley, New York (1928).

Lee, M. K., "Method for Measuring Wavelength and Bursting Period of Flow Oriented Eddies in the Viscous Sublayer," M. S. thesis, Univ. Ill., Urbana (1972).

Levich, V. G., *Physicochemical Hydrodynamics*, Prentice-Hall, Englewood Cliffs, N.J. (1962).

Lin, C. S., E. B. Denton, H. S. Gaskill, and G. L. Putnam, "Diffusion-Controlled Electrode Reactions," *Ind. Eng. Chem.*, **43**, 2136 (1951).
Linton, W. H., and T. K. Sherwood, "Mass Transfer From Solid Shapes to Water in Streamline and Turbulent Flow," *Chem. Eng. Progr.*, **46**, 258 (1950).
McConaghy, G. A., "The Effect of Drag Reducing Polymers on Turbulent Mass Transfer," Ph.D. thesis, Univ. Ill., Urbana (1974).
Mizushina, T., F. Ogino, Y. Oka, and H. Fukuda, "Turbulent Heat and Mass Transfer Between Wall and Fluid Streams of Large Prandtl and Schmidt Numbers," *Intern. J. Heat Mass Transfer*, **14**, 1705 (1971).
Monin, A. S., and A. M. Yaglom, *Statistical Fluid Mechanics; Mechanics of Turbulence*, The M.I.T. Press, Cambridge, Mass. (1965).
Newson, J. D., and A. C. Riddiford, "Limiting Currents for the Reduction of the Tri-iodide Ion at a Rotating Platinum Disk Cathode," *J. Electrochemical Soc.*, **108**, 695 (1961).
Schutz, G., "Untersuchung des Stoffaustausch-Anlaufgebietes in einem Rohr bei Vollausgebildeter Hydrodynamischer Strömung mit einer Elektrochemischen Methode," *Intern. J. Heat Mass Transfer Ser.*, **7**, 1077 (1964).
Shaw, D. A., "Mechanism of Turbulent Mass Transfer to a Pipe Wall at High Schmidt Number," Ph.D. thesis, Univ. Ill., Urbana (1976).
———, and T. J. Hanratty, *AIChE J.*, **23**, No. 2 (1977).
Shaw, D. A., "Measurement of Frequency Spectra of Turbulent Mass Transfer Fluctuations at a Pipe Wall," M.S. thesis, Univ. Ill., Urbana (1973).
Sirkar, K. K., and T. J. Hanratty, "Relation of Turbulent Mass Transfer to a Wall at High Schmidt Numbers to the Velocity Field," *J. Fluid Mech.*, **44**, 589 (1970).
Son, J. S., "Limiting Relation for the Eddy Diffusivity Coefficient Close to a Wall," M.S. thesis, Univ. Ill., Urbana (1965).
———, and T. J. Hanratty, "Limiting Relation for the Eddy Diffusivity Close to a Wall," *AIChE J.*, **13**, 689 (1967).
Theory of the Flowrator, Catalog Section 98-A, Fisher and Porter Co., Hatboro, Pa. (1947).
Van Shaw, P., "A Study of the Fluctuations and the Time Average of the Rate of Turbulent Mass Transfer to a Pipe Wall," Ph.D. thesis, Univ. Ill., Urbana (1963).
Vulterin, J., and J. Zyka, "Investigation of Some Hydrazine Derivatives as Reductimetric Titrants," *Talanta*, **10**, 891 (1963).

Manuscript received May 27, 1976; revision received October 6 and accepted October 8, 1976.

Vortex Free Downflow in Vertical Drains

NORTON G. MCDUFFIE

Chemical Engineering Department
The University of Calgary
Calgary, Alberta T2N 1N4
Canada

Performance of flush drains in gas-liquid separators has been evaluated under conditions of variable gas flow and pressure, liquid height and flow rate, and drain diameter. For the two-phase flow regime, liquid flow rate is found to be independent of vessel pressure or gas flow rate. Transition from weir control to orifice control of liquid flow rate occurs over the range of H/D ratios from 0.4 to 1.5. In this range, simple orifice equations do not apply. Revised design equations for use to determine minimum liquid height for maintenance of single-phase downflow in gas-liquid separators are presented.

SCOPE

Downflow of liquid from a process vessel presents several design problems as outlined by Simpson (1968). The whole downcomer system should be designed to minimize cavitation problems, both in free flow and pumped systems (Anderson et al., 1971; Simpson, 1968). This consideration generally determines dependent values of drain diameter and required head in the process vessel, whether it be predominantly pressure or hydraulic head. A consequent requirement in most processes is that the height of the lower phase (phase 1, Figure 1) be sufficient to repress coning and subsequent mixing of phases (phases 1 and 2, Figure 1); if the second phase is gas, this is especially crucial for vessels supplying liquid to centrifugal pump suctions. Vortex flow and subsequent entrainment can be restricted by installation of cross baffles or vanes in the downcomer mouth. After this precaution is taken, the minimum height H of the lower phase is determined by requirements for stable, vortex free downflow. The study discussed herein was undertaken to attempt to verify and extend bases suggested by Simpson (1968) for determination of minimum lower-phase levels for vessel and drain design.

CONCLUSIONS AND SIGNIFICANCE

This study shows that for a pressurized gas-liquid separator drain system, the maximum attainable steady state liquid superficial velocity V is a function of H/D alone, even in the two-phase flow region (low viscosity liquid). An increase in gas pressure and gas downflow rate does not affect V in the two-phase region. At H/D values from 0.4 to 3, the transition from full liquid flow to two-phase flow occurs at Froude numbers given by the relationship $1.6\,(H/D)^2 \leq Fr \leq 5.1(H/D)^2$. The same relationship applies to liquid superficial Froude numbers attained in two-phase downflow. The transition relationship essentially corroborates Simpson's assumption (1968) utilizing Kalinske's equation (1941) for free downflow with a constant discharge coefficient. The Harleman theoretical